ECS Journal of Solid State Science and Technology, **5** (11) Q3050-Q3053 (2016)
2162-8769/2016/5(11)/Q3050/4/$33.00 © The Electrochemical Society

JSS Focus Issue on Properties, Devices, and Applications Based on 2D Layered Materials

The Effect of Low Energy Ion Implantation on MoS_2

Ryan Murray,[a,z] Katherine Haynes,[a] Xueying Zhao,[a] Scott Perry,[a] Christopher Hatem,[b] and Kevin Jones[a]

[a]*Department of Materials Science and Engineering, University of Florida, Gainesville, Florida 32611, USA*
[b]*Applied Materials, Gloucester, Massachusetts 01930, USA*

The use of ultra low energy ion implantation is investigated as a doping method for MoS_2. 200 eV Cl and Ar implants at doses between 1×10^{13} and 1×10^{15} cm^{-2} were introduced into exfoliated MoS_2 flakes. XPS results for Cl implants show a decrease in core peak binding energies for Mo3d and S2p with increasing dose, implying a p-doping effect. Implantation of MoS_2 device channel regions is shown to reduce the channel's conductivity. However, isolated implantation of the contact region with low doses (1×10^{13} cm^{-2}) of Cl and Ar are shown to improve output characteristics by linearizing the I_{DS}-V_{DS} curves and by increasing current through the device. Cl was shown to be more effective than Ar at increasing the current, implying there is a potential chemical effect as well as damage effect. For higher doses ($\geq 1 \times 10^{14}$ cm^{-2}), the current through the device is reduced with increasing dose for both implant species. This report presents the as-implanted, unannealed results. Post-implantation anneals may be necessary to activate the dopants and fully realize the potential of this doping method.
 [DOI: 10.1149/2.0111611jss]

Manuscript submitted May 23, 2016; revised manuscript received July 18, 2016. Published August 2, 2016. *This paper is part of the JSS Focus Issue on Properties, Devices, and Applications Based on 2D Layered Materials.*

Molybdenum disulfide (MoS_2) and other two-dimensional materials have garnered significant interest in recent years as they have the potential to play important roles in future microelectronics. These materials offer numerous properties that may alleviate issues plaguing the continuation of Moore's Law, including enhanced resistance to short-channel-effects.[1] Additionally, MoS_2 offers unique properties such as a bandgap that changes with the number of layers, and a bandgap that shifts from indirect to direct as the number of layers shrinks to one.[2] Combined with properties such as high flexibility, unique electronic and optoelectronic applications emerge.[3]

A number of issues remain with MoS_2 and other 2D materials that are currently preventing their widespread adoption. Chief among these issues is a large contact resistance, caused by the creation of a non-negligible Schottky barrier that forms due to Fermi-level pinning at the metal/MoS_2 interface.[1] As channel lengths continue to decrease, this issue becomes more prominent as the large contact resistance dominates the overall device resistance. As a means of reducing contact resistance, a number of doping methods have been reported in literature, though these methods are typically unconventional due to the unique situation of dealing with a 2D film. One such method is the use of solution-based chlorine, where it's believed the doping is achieved by filling pre-existing sulfur vacancies with chlorine by exposing the MoS_2 to a solution of dichloroethane.[4]

Ion-implantation is commonly used for conventional bulk semiconductors but has been avoided with 2D materials due to the difficulty in implanting into such thin films. Despite this difficulty, Nipane et al. have recently reported the successful p-doping of MoS_2 with phosphorous using plasma immersion ion implantation (PIII), where the MoS_2 is exposed to a phosphine plasma and bias of 0 eV, 1 keV, or 2 keV is applied to the sample to induce implantation.[5] While plasmas offer benefits such as a wide range of dopant species through different plasma chemistries, it's noted that the plasmas can bring numerous processing difficulties including undesired etching of the MoS_2, imprecise dose control, and degradation of photoresist masks that are used for selective-area doping.

Reports have shown that irradiation of MoS_2 can create sulfur vacancies, which have themselves been shown to have a metallic character and enhanced STM tunneling current relative to the pristine surface.[6] As McDonnell et al. report, the current traveling from a metal contact into the MoS_2 surface can be deconvolved into a linear sum of the current flowing into the pristine surface and the current flowing into naturally-occurring sulfur vacancies.[7] Models predict that even low areal densities (0.1%) of these defects results in a large increase in current through the surface. Thus ion-implantation into MoS_2 offers two potential avenues for doping: the creation of surface sulfur vacancies, and the contribution from the actual implanted dopant species.

In this paper we investigate low energy ion implantation into mechanically exfoliated MoS_2 flakes without exposing the MoS_2 to a plasma. Specifically, we focus on the effect of implantation on the output characteristics of MoS_2 devices, as a function of both dose and implant species. Devices were implanted either into the channel only, or into the contact-region only. No dopant activation anneals were performed, hence this report depicts the initial results of an ongoing investigation.

Results and Discussion

Chlorine and argon were chosen as the implant species due to chlorine's aforementioned reported success as an n-type dopant and argon's chemical inertness, allowing for a comparison of dopant and damage effects. Implants were done at normal incidence. SRIM Monte Carlo simulations were performed to aim for a projected range of 9 Å, or approximately the middle to upper region of the second MoS_2 sheet. This resulted in an implantation energy of 200 eV. With an appropriate dose being largely unknown for this system, a dose matrix of 1×10^{13}, 1×10^{14}, and 1×10^{15} cm^{-2} was used.

To explore the effect of ion implantation on the local structure of MoS_2, X-ray photoelectron spectroscopy (XPS) was performed on bulk mineralogical samples implanted with the same array of Cl doses as the exfoliated flakes used for making devices. Figure 1a shows the Mo 3d and S 2p core peaks for implanted samples as well as for pristine MoS_2. Increasing Cl doses induced core peak shifts to lower binding energies (Figure 1b) as well as broadening of the peaks. The shift in binding energies is consistent with previous reports of preferential sputtering of sulfur atoms from MoS_2 by Ar^+ bombardment.[8,9] In addition, the 1×10^{15} cm^{-2} sample exhibits a MoO_x peak, indicating some oxidation of active Mo sites following implantation. Implantation and subsequent processes were performed in separate tools so post-implantation exposure to air was unavoidable in the test setup.

To confirm the placement of the Cl within the flake, Dynamic SIMS was performed on implanted (200 eV implant energy, 1×10^{13} cm^{-2} dose) MoS_2 films on SiO_2 that were grown by a reported sulfurization of Mo process.[10] This growth method produces films that vary from 3–5 layers in thickness. These films are being used for other experiments and thus their results are not reported here, however the

[z]E-mail: rpmurray@ufl.edu

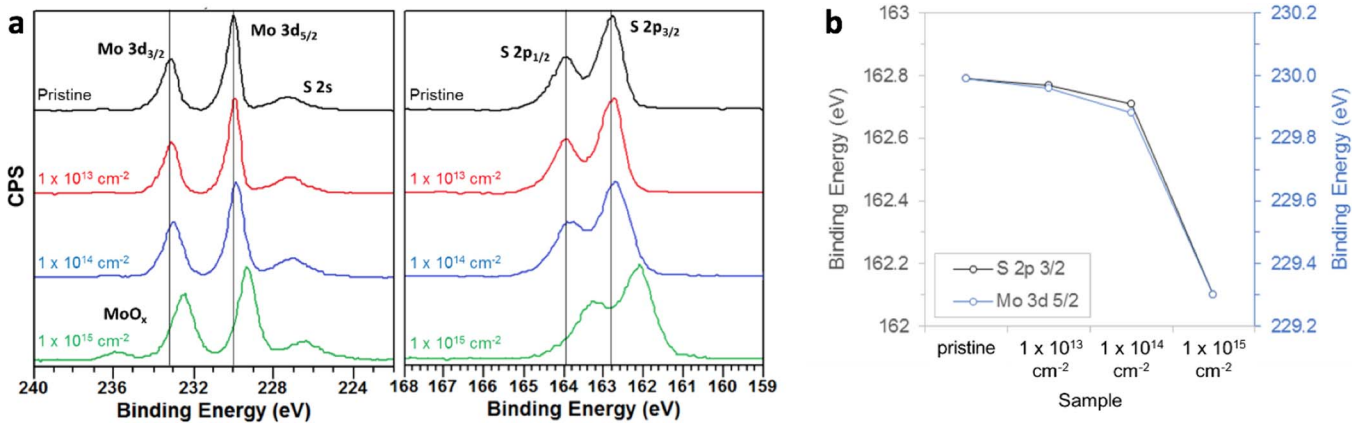

Figure 1. (a) XPS analysis of the pristine and implanted bulk mineralogical MoS_2 shows broadening of the peaks and (b) decreasing binding energy with increasing Cl^+ dose.

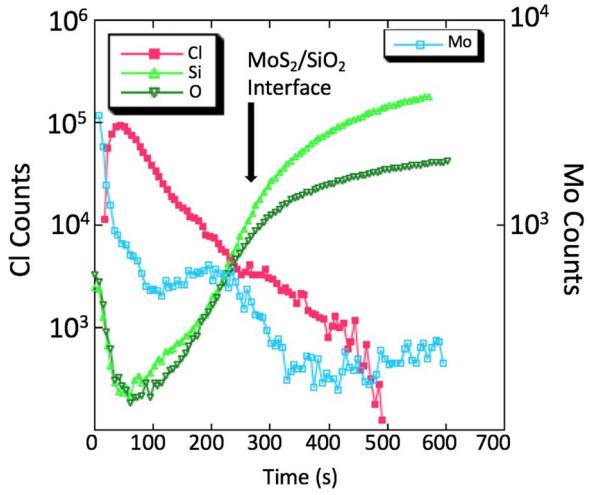

Figure 2. SIMS results for a 3–5 layer-thick grown MoS_2 film on SiO_2 after implantation with a 1×10^{13} cm^{-2} dose of Cl at an implant energy of 200 eV, confirming implantation into the top layers of the MoS_2.

relevant SIMS data (Figure 2) clearly shows the peak Cl concentration within the upper layers of the MoS_2 film. This is in agreement with reported data for the plasma immersion ion implantation of phosphorous into MoS_2, which confirmed the accuracy of SRIM calculations for implantation depth into MoS_2.[5] If the Cl was implanted largely into the oxide it could conceivably cause an electrostatic effect on the MoS_2, however given the SIMS data such an electrostatic effect would be expected to be insignificant. Notably, without a reference MoS_2 sample containing a known Cl concentration it is not possible to determine a Cl concentration from our SIMS data nor is it appropriate to directly compare counts of the different species.

Naturally occurring MoS_2 purchased from SPI was mechanically exfoliated onto 300 nm SiO_2 on Si substrates. Flakes of appropriate thickness were identified based on their optical contrast, with few-layer thick flakes (~5-15 layers) being targeted due to their reported higher on-currents when compared to mono- or many-layered flakes.[11,12] All devices were fabricated using a conventional maskless photolithography process flow. While Ti contacts have been shown to produce relatively good contacts to MoS_2, the contacts in this experiment were chosen to be Ni/Au (30/90 nm) due to titanium's tendency to getter our implant species, chlorine.[4] For the channel-implanted devices (Figure 3a), the electrical properties were measured after device fabrication, then the samples were implanted (the metal contacts prevented the contact-area from implantation), and the electrical properties were measured again. This allowed for a direct before- and after-implantation comparison. For the contact-region implanted devices (Figure 3b), implantation was performed after lithographic patterning and photoresist development, but before metal contact deposition. This allowed for the 800 nm of photoresist to protect the channel from implantation. However, it does not allow for a direct comparison between before- and after-implantation for a single device, so all comparisons are made for devices with similar channel

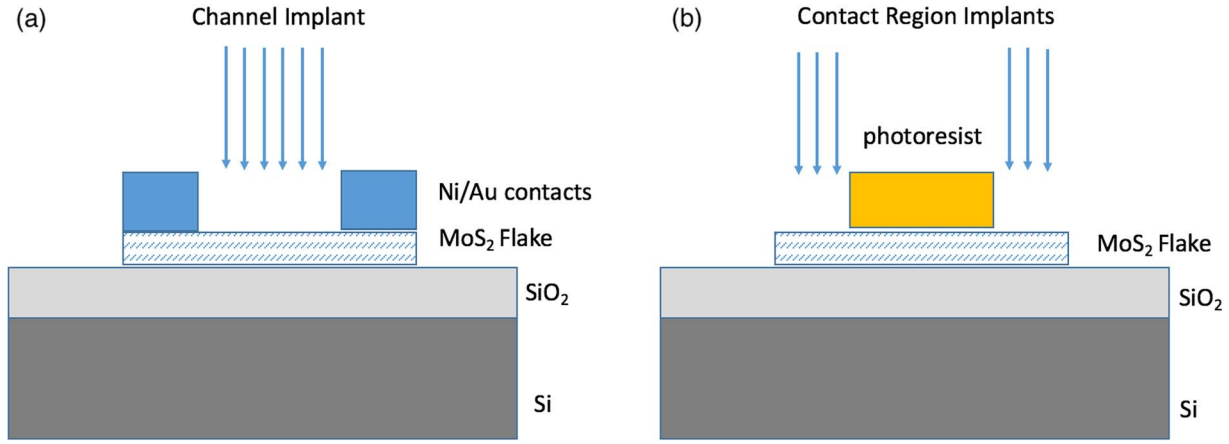

Figure 3. A depiction of the two types of implantations performed, isolated channel implantations (a) and isolated contact region implants (b).

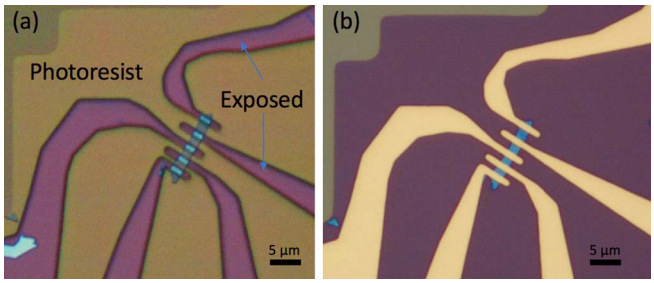

Figure 4. Optical microscope images depicting the process flow for contact-region implanted samples. Photolithographic patterning was used to define the device channels (a). Implantation was performed after (a) and prior to metal contact deposition, with the photoresist protecting the channel during implantation. (b) depicts a typical completed device on a few-layer MoS_2 flake.

lengths and flake thicknesses. An example of the process flow for fabrication of the contact-region implanted samples is provided in Figure 4. Unless otherwise stated, no anneals were performed on any of the devices. Measurements were performed in air, and no device gating or transfer characteristics were investigated.

Prior to implantation, our MoS_2 devices on few-layer flakes typically produced a non-linear I_{DS}-V_{DS} response (Figure 5), representative of Schottky behavior at the metal/MoS_2 interface. Following implantation of the channel with chlorine, I_{DS}-V_{DS} characteristics remained non-linear but a decrease in current was observed. An example is shown in Figure 5 for the 1×10^{13} cm^{-2} Cl dosed sample, which experienced a nearly 5× decrease in current after implantation, a typical result for that dose. The higher doses produced similar results but with the reduction in current being >100×. With such a reduction in current observed after implanting the channel, argon was not investigated as a species for channel implantation.

The data for the contact-region implanted samples is summarized in Table I. The 1×10^{13} cm^{-2} dose for both Cl and Ar contact-region implants produced linear I_{DS}-V_{DS} output characteristics (Figure 6), in contrast to the non-linear results of unimplanted samples. Compared to the unimplanted sample, the current increased by 4× for the Cl implantation. Similar to the Cl implant, the 1×10^{13} cm^{-2} Ar dosed sample also yielded an increase in current over the unimplanted sample, though it was an increase of only 2×, half that of the Cl implant.

Like the 1×10^{13} cm^{-2} dose, the 1×10^{14} cm^{-2} Cl dose for the contact-region implantations yielded linear I_{DS}-V_{DS} curves. However,

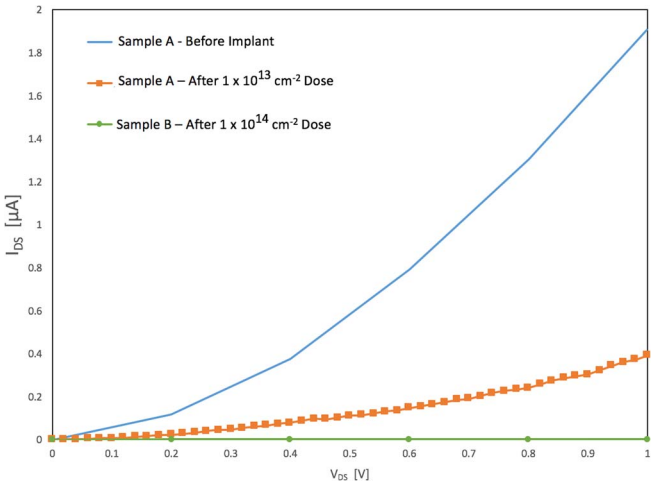

Figure 5. Output characteristics for before and after implantation of the channel with a 1×10^{13} cm^{-2} dose of Cl (Sample A), and a typical high resistance result after implantation of the channel with 1×10^{14} cm^{-2} dose of Cl (Sample B). A nearly 5× reduction in current is observed after implantation of the channel with a 1×10^{13} cm^{-2} dose of Cl (Sample A).

Table I. Drain current ($V_D = 1$ V) for the contact-region implanted samples.

Implant Species	Implant Dose [cm^{-2}]	$I_D(V_D = 1\ V)$ [μA/μm]
Cl	1×10^{13}	4.32
Ar	1×10^{13}	1.93
Unimplanted	Unimplanted	1.08
Cl	1×10^{14}	0.64
Ar	1×10^{14}	0.52

this implant resulted in a decrease in current when compared to both the 1×10^{13} cm^{-2} Cl dose (6.75× reduction) and the unimplanted sample (1.5× reduction). The 1×10^{14} cm^{-2} Ar doses into the contact-region, however, produced less reliable results. The output characteristics displayed a variety of linear, non-linear, and non-conducting I_{DS}-V_{DS} curves. For a device yielding linear output characteristics, a current of 0.52 μA/μm was observed ($V_{DS} = 1$ V, channel length = 1 μm), which is close to the 0.64 μA/μm observed for the 1×10^{14} cm^{-2} Cl dosed sample. As reported in literature, a large increase in current would be expected for all samples measured here after the deposition of a high-k dielectric over the devices.[13]

The 1×10^{15} cm^{-2} dosed samples for both Cl and Ar produced highly resistive devices and were excluded from further analysis, likely due to the surface oxidation observed in XPS (Figure 1a).

The decrease in core peak binding energy observed with increasing dose in the XPS data is typically indicative of p-type doping,[5] in contrast to the expected n-type doping of the Cl implant.[4] However, as no anneals were performed, the activation of the dopant is undetermined. As MoS_2 is naturally n-type, a compensating p-doping would explain the reduction in current observed with the channel implantations. However, this would not explain the linearization of the output characteristics with low-dose implantation into the contact-region. Literature has reported the formation of sulfur vacancies and other defects upon ion bombardment, and models have correlated an increase in density of sulfur vacancies with an increase in current through a metal/ MoS_2 interface.[6,7] This suggests that the defects induced by implantation create an altered metal/MoS_2 interface that yields a reduction in the Schottky barrier and linearizes the output characteristics.

The as-implanted, unannealed data presented here allows for a comparison to the reported chlorine doping of MoS_2, where no annealing was needed or performed in order to produce a doping effect after exposure of MoS_2 to a chlorine-containing solution.[4] For that study it was not confirmed whether the Cl substituted sulfur or was adsorbed. However, the authors believed the observed n-type doping was indicative of sulfur substitution rather than adsorption. Such observations and conclusions are in agreement with multiple reports:

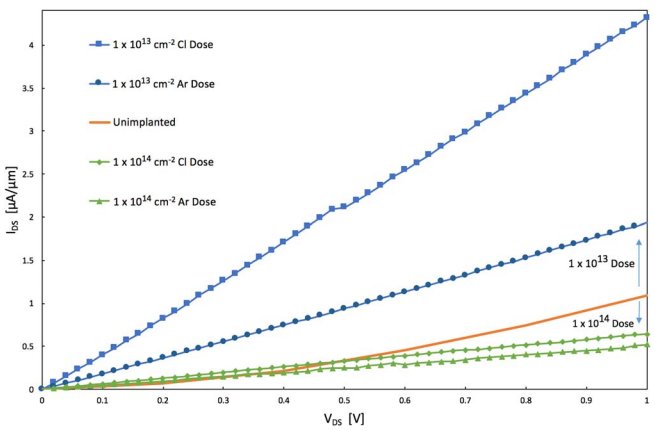

Figure 6. Output characteristics of contact-region implanted MoS_2 devices with a channel length of 1 μm.

p-type doping observed from halogens on the MoS_2 surface, where the high electronegativity of the halogen draws electrons from the MoS_2 and induces p-type doping; and DFT calculations that suggest Cl substituted on a sulfur site will partially donate its unpaired electron to Mo, despite the high electronegativity of Cl.[14,15] While irradiation damage has been shown to have a p-type effect on MoS_2, if the implants in our study were not activated and were located within the Van der Waals gap then the observed doping compensation and corresponding reduction in drain current after channel implantation could also be explained by the aforementioned reported p-type doping of adsorbed halogens.[8,9]

Additionally, while the DFT study indicated a comparable formation energy for the adsorption of Cl and for its substitution onto a sulfur site, it also showed that the energy difference between the two formation routes should theoretically depend on the abundance of sulfur.[15] The authors suggested it might therefore be possible to induce substitution rather than adsorption by using MoS_2 that has an increased amount of sulfur vacancies. Since irradiation of MoS_2 can induce the formation of sulfur vacancies, this might imply ion implantation of MoS_2 is less dependent on annealing for dopant activation when compared to the implantation of traditional bulk semiconductors.[6] Our results, however, indicate annealing is likely required to activate the dopants.

Conclusions

Low-energy ion implantation of few-layer MoS_2 flakes was studied. 200 eV Cl and Ar implants result in a 9 Å projected range, approximately at the top of the second MoS_2 layer. Prior to implantation, non-linear device output characteristics were typically observed. After implantation of chlorine into the channel of a device, a reduction in current of $\sim 5\times$ was observed for a dose of 1×10^{13} cm^{-2}, while higher doses yielded a $>100\times$ reduction. This is likely due to compensation of the naturally n-type MoS_2 by p-type doping as observed in the red shifts of the Mo 3d and S 2p core peaks in the XPS data, induced either by implantation damage or by unactivated implants within the Van der Waals gap. Low-dose (1×10^{13} cm^{-2}) implantations isolated into the contact-region produced linear I_{DS}-V_{DS} results instead of Schottky I_{DS}-V_{DS} behavior for both Cl and Ar implant species. This is suspected to be caused by enhanced out-of-plane current transport due to implantation-induced defects. Cl contact-region implants produced devices with $\sim 2\times$ higher current compared to Ar implants, implying a chemical effect in addition to damage effect of the implanted species. Post-implantation annealing studies are required to determine the complete effect of this doping method.

Acknowledgments

The authors thank Niloy Mukherjee and Intel/SRC for funding and resources, as well as the engineers at the Nanoscale Research Facility at the University of Florida, Max Lemaitre, and Andrew Rinzler for all their help. We would also like to thank Mikhail Klimov for help with the SIMS data and IMEC for the grown MoS_2 films.

References

1. H. Liu, A. T. Neal, and P. D. Ye, *ACS Nano*, **6**(10), 8563 (2012).
2. A. Kuc, N. Zibouche, and T. Heine, *Physical Review B*, **83**(24), 245213 (2011).
3. J. Pu, Y. Yomogida, K.-K. Liu, L.-J. Li, Y. Iwasa, and T. Takenobu, *Nano Letters*, **12**(8), 4013 (2012).
4. L. Yang, K. Majumdar, H. Liu, Y. Du, H. Wu, M. Hatzistergos, P. Y. Hung, R. Tieckelmann, W. Tsai, C. Hobbs, and P. D. Ye, *Nano Letters*, **14**(11), 6275 (2014).
5. A. Nipane, D. Karmakar, N. Kaushik, S. Karande, and S. Lodha, *ACS Nano*, **10**(2), 2128 (2016).
6. A. Inoue, T. Komori, and K.-I. Shudo, *Journal of Electron Spectroscopy and Related Phenomena*, **189**, Supplement 11 (2013).
7. S. McDonnell, R. Addou, C. Buie, R. M. Wallace, and C. L. Hinkle, *ACS Nano*, **8**(3), 2880 (2014).
8. M. Quan, M. O. Patrick, M. John, L. Duy, S. W. Chen, Z. Yeming, C. Tianyang, S. Dezheng, Y. Koichi, T. Tai, W. Michelle, L. M. Jessica, W. Jonathan, M. KatieMarie, F. H. Tony, S. R. Talat, K. Roland, and B. Ludwig, *Journal of Physics: Condensed Matter*, **25**(25), 252201 (2013).
9. M. A. Baker, R. Gilmore, C. Lenardi, and W. Gissler, *Applied Surface Science*, **150**(1–4), 255 (1999).
10. D. Chiappe, I. Asselberghs, S. Sutar, S. Iacovo, V. Afanas'ev, A. Stesmans, Y. Balaji, L. Peters, M. Heyne, M. Mannarino, W. Vandervorst, S. Sayan, C. Huyghebaert, M. Caymax, M. Heyns, S. De Gendt, I. Radu, and A. Thean, *Advanced Materials Interfaces*, **3.4**, 1500635 (2015).
11. H. Li, J. Wu, X. Huang, G. Lu, J. Yang, X. Lu, Q. Xiong, and H. Zhang, *ACS Nano*, **7**(11), 10344 (2013).
12. W. Liu, J. Kang, W. Cao, D. Sarkar, Y. Khatami, D. Jena, and K. Banerjee, in "*2013 IEEE International Electron Devices Meeting*", p. 19.14.11–19.14.14 (2013).
13. S. Das, H.-Y. Chen, A. V. Penumatcha, and J. Appenzeller, *Nano Letters*, **13**(1), 100 (2013).
14. D. M. Sim, M. Kim, S. Yim, M. Choi, J. Choi, S. Yoo, and Y. S. Jung, *ACS Nano*, **9**(12), 12115 (2015).
15. A. Carvalho and A. H. Castro Neto, *Physical Review B* **89**(1–5), 081406 (2014).